

# Extended Scaling in High Dimensions

*B. Berche*<sup>1</sup>, *C. Chatelain*<sup>1</sup>, *C. Dhall*<sup>2</sup>,  
*R. Kenna*<sup>1,2</sup>, *R. Low*<sup>2</sup>, and *J.-C. Walter*<sup>1</sup>

<sup>1</sup> Laboratoire de Physique des Matériaux, UMR CNRS No. 7556,  
Université Henri Poincaré (Nancy 1), B.P. 239,  
F-54506 Vandœuvre lès Nancy cedex, France

<sup>2</sup> Applied Mathematics Research Centre, Coventry University,  
Coventry, CV1 5FB, England

September 12, 2021

## Abstract

We apply and test the recently proposed “extended scaling” scheme in an analysis of the magnetic susceptibility of Ising systems above the upper critical dimension. The data are obtained by Monte Carlo simulations using both the conventional Wolff cluster algorithm and the Prokof’ev-Svistunov worm algorithm. As already observed for other models, extended scaling is shown to extend the high-temperature critical scaling regime over a range of temperatures much wider than that achieved conventionally. It allows for an accurate determination of leading and sub-leading scaling indices, critical temperatures and amplitudes of the confluent corrections.

# 1 Introduction

An approach to critical-point scaling motivated by high-temperature series expansions has recently been developed, which aims to extend the scaling window well beyond the critical regime [1]. At a temperature  $T$  sufficiently close to the critical temperature  $T_c$ , divergent thermodynamical averages display the scaling behavior  $O(T) \approx A_O t^{-\rho}$  where  $A_O$  is a constant amplitude,  $\rho$  is the critical index associated with the observable  $O$  and  $t = (T - T_c)/T_c$  is the standard reduced temperature. In order to improve the temperature range where scaling holds, other thermal scaling variables have been considered in the literature. In particular the alternative reduced temperature

$$\tau = \frac{T - T_c}{T} = \frac{\beta_c - \beta}{\beta_c} \quad (1.1)$$

is popular in analysis of series expansions. This variable is also natural in renormalization group analyses where the temperature variable usually appears through  $\beta J$  ( $J$  being a coupling constant between microscopic degrees of freedom), and thus the reduced variable is defined as in (1.1). The relationships between the two reduced temperatures are

$$t = \frac{\tau}{1 - \tau} = \tau + \tau^2 + \tau^3 + \dots, \quad (1.2)$$

$$\tau = \frac{t}{1 + t} = t - t^2 + t^3 - \dots, \quad (1.3)$$

such that in the vicinity of the critical point

$$O(T) \approx A_O t^{-\rho} \quad \text{or} \quad O(T) \approx A_O \tau^{-\rho}. \quad (1.4)$$

While both  $t$  and  $\tau$  vanish as the critical point is approached, they have very different high-temperature limits,

$$\lim_{T \rightarrow \infty} t = \infty, \quad (1.5)$$

$$\lim_{T \rightarrow \infty} \tau = 1. \quad (1.6)$$

In [1], a rationale was given explaining why the alternative reduced temperature  $\tau$  in (1.1) may be superior to the more traditional variable  $t$  in scaling analyses, at least in the high-temperature regime. This rationale stems from the following observations. Firstly, suppose the constant  $A_O$  in (1.4) is promoted to a temperature-dependent amplitude as follows,

$$O(T) \propto O^*(T) \sim T^{\psi_O} (T - T_c)^{-\rho} \sim T^{\psi_O - \rho} \left(1 - \frac{T_c}{T}\right)^{-\rho} \sim \beta^{\phi_O} \tau^{-\rho}, \quad (1.7)$$

where  $\phi_O = \rho - \psi_O$ . From (1.6),

$$\lim_{T \rightarrow \infty} O^*(T) \sim \beta^{\phi_O}, \quad (1.8)$$

and  $\phi_O$  may be chosen so that  $O^*(T)$  matches the high-temperature series expansion (HTSE) for  $O(T)$  in this limit. Note that a similar approach cannot be implemented for scaling in  $t$ . I.e., scaling in  $\tau$ , unlike scaling in  $t$ , allows  $O^*(T)$  to represent the correct asymptotic behavior of  $O(T)$  in the  $T \rightarrow \infty$  limit as well as close to criticality. Inspired by (1.7) we now write the full expression for the observable  $O(T)$  as

$$O(T) = A_O O^*(T) = A_O \beta^{\phi_O} \tau^{-\rho} + \dots, \quad (1.9)$$

where the dots represent higher-order additive corrections.

In [1, 2], Campbell et al. proposed and tested the extended scaling scenario in the Ising model in two dimensions as well as the Ising, Heisenberg and XY models in  $d = 3$  dimensions. These works convincingly established the superiority of the method over the conventional scheme between the lower and upper critical dimensions. The inherent idealness of the extended scaling approach to study systems *below* the lower critical dimension was demonstrated in [3]. In this work, we test extended scaling for the  $d$ -dimensional Ising models with  $d = 5, 6, 7$  and  $8$ , i.e. *above* the upper critical dimension  $d_c = 4$ . Furthermore, while the  $d \rightarrow \infty$  (mean-field) case was also investigated in [2] (where extended scaling is exact for all  $T > T_c$ ), here we include a detailed analysis of corrections in the extended scaling scheme.

In the next section we review the known results about the leading and sub-leading scaling behavior of the Ising model above  $d_c$ . We then define the extended scaling of this model, taking into account scaling corrections. In Section 3 the MC approach is presented and in Section 4 the resulting data is discussed. Agreement with results from HTSE confirms the efficacy of extended scaling, which is then used to determine the critical parameters governing scaling in higher dimensions. Since above  $d = 6$  dimensions, the dominant corrections to scaling are due to analytic terms, this work provides a full account of leading and confluent corrections in the susceptibility above the upper critical dimension. We conclude in Section 5.

## 2 Extended scaling in high dimensions

Above the upper critical dimension  $d_c = 4$ , the leading scaling behavior for the magnetic susceptibility is given by mean field theory and is characterized by the exponent  $\gamma = 1$ . The additive correction-to-scaling terms are expected to be non-classical. The generic scaling form for the reduced susceptibility for the Ising model is

$$\chi(T)/\beta = \Gamma t^{-\gamma} \left( 1 + b_1 t^\theta + b_2 t^{2\theta} + \dots + c_1 t + c_2 t^2 + \dots \right), \quad (2.1)$$

where the dots indicate higher-order terms. In (2.1), the confluent (or non-analytic) corrections involve the universal exponent  $\theta$ , while the remaining correction terms are analytic. (While in principle there could be several confluent correction exponents involved in (2.1), it is sufficient in this work to consider the single exponent  $\theta$ .) Analysis of the  $\phi^4$  model above  $d_c = 4$  shows that the dominant critical behavior is determined by the Gaussian fixed point, leading to  $\chi \approx \langle \phi^2 \rangle \approx t^{-1}$  and  $\xi \approx t^{-1/2}$ . The confluent scaling

Table 1: Selection of previous estimates for the critical temperature  $T_c$  for high-dimensional Ising models together with the refined extended scaling estimates obtained in Sec. 4 of this paper. Here, FSS means a Monte Carlo approach using finite-size scaling.

Reference method & year	$T_C$ $d = 5$	$T_C$ $d = 6$	$T_C$ $d = 7$	$T_C$ $d = 8$
[8] $1/d$ expansion (1964)	8.7881...	10.8397...	12.8712...	14.8923...
[4] (critical expansion) (1981)	8.8162(5)	10.8656(8)		
[7] HTSE (1993)	8.777(2)			
[6] HTSE (1993)		10.8348(4)	12.8690(4)	
[9] FSS (1999)	8.77844(2)			
[10] FSS (2000)		10.835(5)		
[11] FSS (2001)			12.870(5)	
[12] FSS (2005)	8.7785(5)			
[13] FSS (2006)			12.870(5)	14.893(3)
This paper (2008)	8.7777(9)	10.8353(4)	12.8690(3)	14.8933(8)

corrections are due to the irrelevant  $\phi^4$  term. The perturbation felt by the system inside the correlation volume is  $\langle \phi^4 \rangle / \xi^d \approx \langle \phi^2 \rangle^2 / \xi^d$  (since the average is taken over a Gaussian distribution), which thus behaves in the vicinity of the critical point as  $\chi^2 / \xi^d \approx t^{-2+d/2}$ . As a consequence, the exponent  $\theta$  is given by

$$\theta = \frac{d-4}{2} \quad (2.2)$$

for  $d > d_c = 4$ . Thus, for  $d > 6$ , where  $\theta > 1$ , the confluent corrections are expected to be overwhelmed by the analytic ones. In six dimensions, the corrections are expected to be modified by a logarithmic factor [4, 5], and, explicitly,

$$\chi(T)/\beta = \Gamma t^{-1} + B t^{-\frac{1}{2}} + C + D t^{\frac{1}{2}} + \dots, \quad \text{for } d = 5, \quad (2.3)$$

$$\chi(T)/\beta = \Gamma t^{-1} + B \ln t + C + D t \ln t + \dots, \quad \text{for } d = 6, \quad (2.4)$$

$$\chi(T)/\beta = \Gamma t^{-1} + C + D t^{\frac{1}{2}} + \dots, \quad \text{for } d = 7, \quad (2.5)$$

$$\chi(T)/\beta = \Gamma t^{-1} + C + D t + \dots, \quad \text{for } d = 8. \quad (2.6)$$

Series analysis techniques have been used to verify the leading correction-to-scaling exponent  $\theta$  in five and six dimensions and to determine some of the critical amplitudes [4]. In particular, accepting the classical value  $\gamma = 1$ , Guttman measured  $\theta = 0.50(5)$ ,  $\Gamma = 1.311(9)$  and  $B = -0.48(3)$  in five dimensions as well as  $\theta = 0.98(5)$  and  $\Gamma = 1.168(8)$  in six dimensions [4]. It was not possible to determine the subdominant amplitudes, nor to confirm the logarithmic term, in six dimensions using these techniques [4].

The high-temperature series expansion (HTSE) for  $d$ -dimensional Ising models was given to fifteenth order in  $\tanh(\beta)$  by Gofman et al. in [6], and compared with results of Monte Carlo simulations in six and seven dimensions. The HTSE in five dimensions

was analyzed in a related study [7]. In contrast to five dimensions where the leading corrections are confluent, analytic corrections to scaling were favored in  $d = 6$  and  $d = 7$  dimensions [6] using the HTSE approach. However, the logarithmic term in six dimensions was also not explicitly handled in the series expansion approach of [6]. With no prior assumptions regarding exponent values, and ignoring the logarithm in six dimensions, the HTSE gave  $\theta = 0.45(10)$ ,  $\theta = 1.0(3)$  and  $\theta = 0.8(2)$  in  $d = 5$ ,  $d = 6$  and  $d = 7$  dimensions, respectively [6, 7]. For convenience, a list of previous measurements of the critical temperatures in high-dimensional Ising models is given in Table 1.

Here, we report on simulations of the Ising model in  $d = 5, 6, 7$  and 8 dimensions using the new extended scaling method recently developed by Campbell et al. [1]. It is claimed that this new method can extend the scaling regime well beyond that traditionally available [1]. This claim has been verified in all models so far tested below their upper critical dimensions [2] and the method is particularly well suited to models which order at zero temperature, i.e., below the *lower* critical dimension [3]. A central theme of this paper is to test the applicability of the method for high dimensions, i.e., above the upper critical dimension, and if it is proven more suitable than “standard temperature scaling”, the method will be used to investigate corrections to scaling and amplitudes beyond the leading critical behaviour.

We consider the magnetic susceptibility  $\chi(T)/\beta$  which is defined in the paramagnetic phase as

$$\chi(T)/\beta = \frac{1}{N} \sum_{i,j} \langle s_i s_j \rangle, \quad (2.7)$$

and numerically estimated by integration of the spin-spin correlation functions over the lattice. With complete randomization in the high-temperature limit ( $T \rightarrow \infty$ ),  $\langle s_i s_j \rangle = \delta_{ij}$  there, so that  $\chi(T)/\beta$  approaches unity. Therefore the HTSE for the reduced susceptibility has the form

$$\chi(T)/\beta = a_0 + a_1\beta + a_2\beta^2 + a_3\beta^3 + \dots, \quad (2.8)$$

where  $a_0 = 1$  for all  $d$ . Comparing this to (1.8), it is clear that  $\phi_\chi = 0$  for the reduced susceptibility. This is the reason why the second equation in (1.4) may represent the susceptibility over an extended high-temperature range. The limit (1.5), on the other hand, restricts the suitability of the conventional variable  $t$  for temperature scaling analysis in the vicinity of the critical point. Writing the five-dimensional critical expansion (2.3) in terms of the extended scaling reduced temperature  $\tau$  instead of  $t$ , one has

$$\chi(T)/\beta = \Gamma\tau^{-1} + B\tau^{-\frac{1}{2}} + C(\tau), \quad (2.9)$$

where the higher corrections are contained in the function  $C(\tau)$ , which goes to a constant  $C$  in the high-temperature limit. Since both  $\tau$  and  $\chi(T)$  approach unity there, one has  $C = 1 - \Gamma - B$ . Similar considerations in six and higher dimensions lead to

$$\chi(T)/\beta \sim \Gamma\tau^{-1} + B \ln(\tau) + C, \quad (2.10)$$

and

$$\chi(T)/\beta \sim \Gamma\tau^{-1} + C, \quad (2.11)$$

respectively, where  $C = 1 - \Gamma$ .

### 3 The Monte Carlo algorithms

The (main) data presented in this work have been obtained using the so-called worm algorithm introduced by Prokof'ev and Svistunov and which provides an efficient Monte Carlo sampling of the dominant terms of the HTSE of spin-spin correlation functions [14, 15]. The data resulting from this approach are labelled MCHTSE (for Monte Carlo high-temperature series expansion) throughout this paper. In the case of the Ising model, this HTSE is

$$\langle s_i s_j \rangle = \frac{1}{\mathcal{Z}} \sum_{\{s\}} s_i s_j e^{\beta \sum_{(k,l)} s_k s_l} = \frac{1}{\mathcal{Z}} (\cosh \beta)^{dN} \sum_{\{s\}} s_i s_j \prod_{(k,l)} (1 + s_k s_l \tanh \beta). \quad (3.1)$$

Here,  $s_i$  is the spin at site  $i$  of the  $d$ -dimensional lattice,  $\mathcal{Z}$  is the partition function, the summation is taken over configurations and  $(k, l)$  denotes a pair of neighboring sites on the lattice. Since  $\sum_{s_i=\pm 1} s_i^{2p} = 2$  while  $\sum_{s_i=\pm 1} s_i^{2p+1} = 0$  for integer  $p$ , the only graphs that contribute to the expansion are paths joining sites  $i$  and  $j$  (which we call sources) and closed loops. These graphs can be sampled stochastically using the following rules: one of the sources, say that initially at site  $i$ , is moved to one of the neighboring sites, say  $i'$ , and a bond is added between  $i$  and  $i'$  if none was hitherto present, or the bond is deleted if already present. If the two sources are on the same site, i.e.  $i = j$ , they are both moved to a new randomly chosen site. These three moves are chosen using a Metropolis prescription: the probability to add a bond is  $\min(1, \tanh \beta J)$ , that to delete a bond is  $\min(1, 1/\tanh \beta J)$  while the probability to move both sources can be set freely. This algorithm is known to be slightly more efficient than Swendsen-Wang cluster algorithm [16]. To accelerate the dynamics, the state of the bonds starting from the same site is stored as a single bit. Furthermore we implemented a continuous-time version of the worm algorithm. At each Monte Carlo step, the probability  $\omega_\alpha$  of all possible moves is calculated. The time  $\tau$  that the system will stay in the same state is evaluated as [17]

$$\tau = 1 + \text{Int} \left( \frac{\ln \eta}{\ln(1 - \sum_\alpha \omega_\alpha)} \right), \quad (3.2)$$

where  $\eta$  is a random variable uniformly distributed over  $]0; 1]$ . The time is increased by  $\tau$  and one of the moves  $\alpha$  is chosen with probability  $\omega_\alpha$  and applied to the system.

As the temperature approaches the critical temperature, the worm algorithm generates graphs contributing to higher and higher orders of the HTSE. The number of these graphs grows exponentially fast which may cause critical slowing-down of the convergence of the averages. To check the results, additional data have been computed using the standard Wolff algorithm [18] whose critical slowing-down is much better understood. For a given lattice size, the simulations have been performed at a temperature close to  $T_c$ , and data for nearby temperatures were obtained by the so-called histogram reweighting method [19]. The reliability of the MCHTSE data is demonstrated in Fig. 1, where estimates for the susceptibility from this method are compared with those from the HTSE of [6] and conventional Monte Carlo data for lattice sizes  $L = 6-14$  in five dimensions. Clearly,

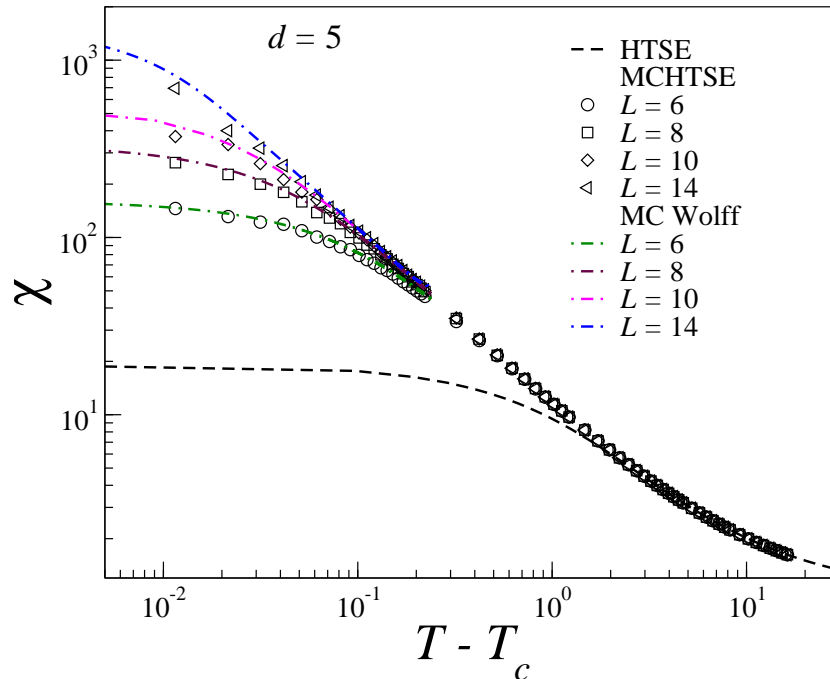


Figure 1: MCHTSE estimates for the susceptibility of the five-dimensional Ising model compared with conventional Monte Carlo estimates (dot-dashed curves, colored online) using the Wolff algorithm together with histogram reweighting and with the HTSE of [6] (dashed line, black online).

the MCHTSE data accurately follow the HTSE curve for large  $T$  and are comparable to conventional MC estimates closer to  $T_c$ , where finite-size effects become important. Furthermore, the MCHTSE for  $L \geq 10$  is independent of  $L$  down to  $T \approx T_c + 0.1 \approx 8.9$ .

## 4 Extended scaling analysis of MC data

Using the numerical approach presented in Sec. 3, we computed the magnetic susceptibility  $\chi$  in Ising models above  $d_c$ . Extended scaling is tested in Figs. 1–7 and then employed to determine the leading corrections for the scaling behavior of the susceptibility. In particular, we firstly determine  $\theta$ ,  $\Gamma$ ,  $B$  and  $C$  in five dimensions. The agreement between our measurements there and those of [4] establishes confidence in the extended scaling approach. The fifteenth-order HTSE for  $d$ -dimensional Ising models of Gofman et al. in [6] is indeed expected to be accurate at sufficiently high temperature, while the critical expansion of Guttman [4] should be reliable close to criticality. Extended Scaling is then used to measure  $\theta$ ,  $\Gamma$ ,  $B$  and  $C$  in six dimensions as well as  $\theta$ ,  $\Gamma$  and  $C$  in seven and eight dimensions. The scaling forms (2.3), (2.4), (2.5) and (2.6) are confirmed (including for the first time the logarithmic correction in the leading correction-to-scaling term in six dimensions) and hence the general formula (2.2) is supported. These forms are then used to determine refined estimates for  $T_c$  in  $d = 5$  to  $d = 8$  dimensions. The amplitude of the logarithm in six dimensions turns out to be small, explaining the difficulties in verifying

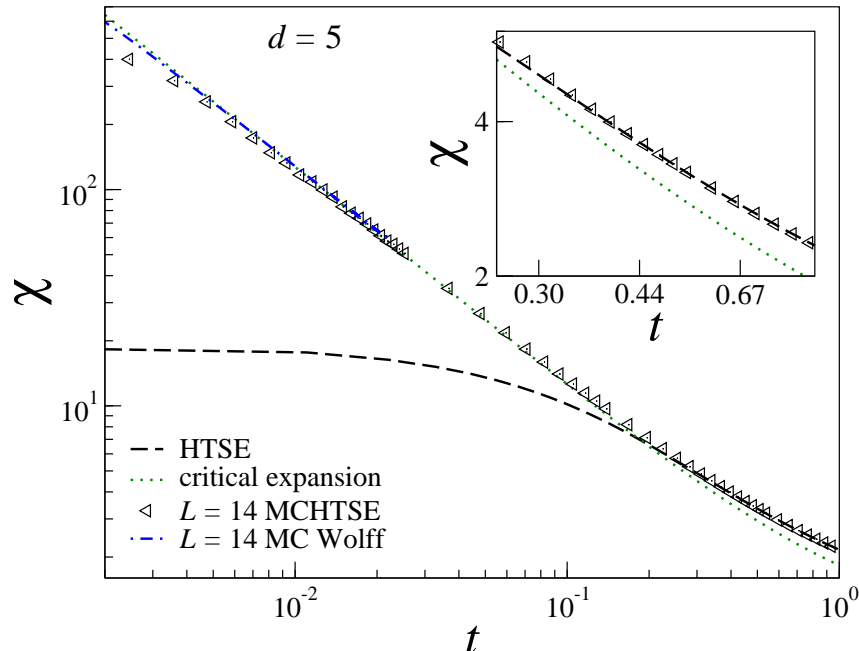


Figure 2: MCHTSE estimates for the susceptibility of the five-dimensional Ising model compared with conventional Monte Carlo estimates (dot-dashed curve, blue online), the HTSE of [6] (dashed line, black) and the critical expansion of [4] (dotted line, green online). The inset illustrates how the critical expansion becomes inaccurate at high temperature where the MCHTSE data cross over to the HTSE curve.

it numerically almost thirty years ago [4].

## 4.1 Five-dimensional case

In Fig. 2, the  $d = 5$ ,  $L = 14$  MCHTSE data are compared with the HTSE [6], the critical expansion [4] and conventional  $L = 14$  MC data on a double-logarithmic scale using the standard reduced temperature  $t$ . The MCHTSE data follow the critical curve for  $t \gtrsim 0.05$  to  $t \lesssim 0.2$ , where they cross over to the HTSE curve. The inset in Fig. 2 is a blow-up of this region, and clearly illustrates the deviation of the critical expansion from the HTSE and the MCHTSE data.

To extract the parameters governing the scaling in five dimensions, the following extended scaling analysis was applied to the MCHTSE data. From (2.3), the first three terms characterizing the critical behavior of the susceptibility are expected to be of the form

$$\chi(T)/\beta \sim \Gamma\tau^{-\gamma} + B\tau^{\vartheta} + C, \quad (4.1)$$

where  $\vartheta = -\gamma + \theta$  from (2.1),  $\tau$  is given in (1.1) and extended scaling gives  $C = 1 - \Gamma - B$ . Firstly, for  $L = 14$ , a six-parameter fit of the MCHTSE data to (4.1) between  $T = 8.9$  and  $T = 25$  gives an estimate for  $T_c$  of 8.7743(95), which compares well with the best estimate in the literature ( $T_c = 8.77844(2)$  [9]). Refined extended scaling estimates for

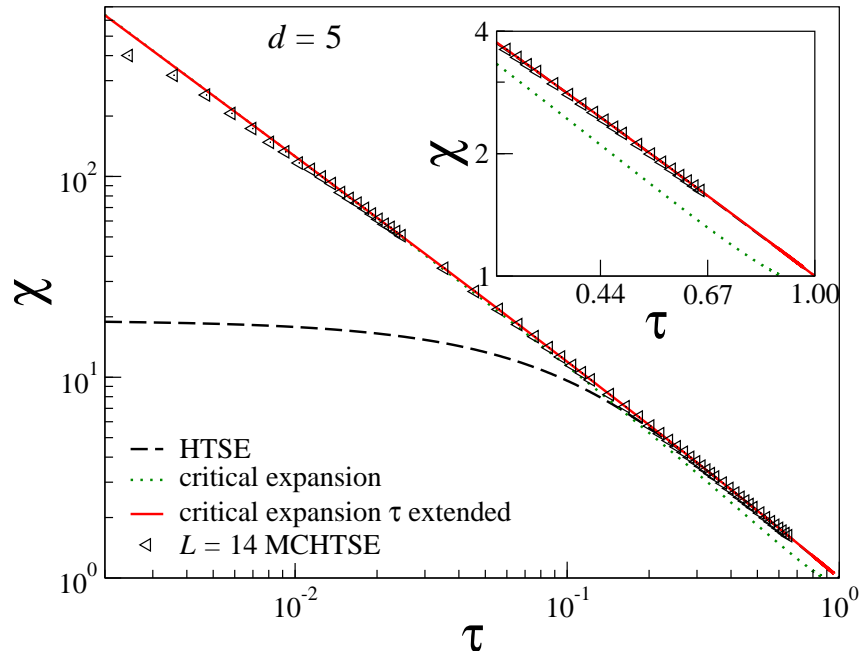


Figure 3: Extended scaling for the susceptibility of the  $d = 5$  Ising model. The extended scaling curve (solid, red online) coincides with the critical curve (dotted, green online) [4] close to  $\tau = 0$  ( $T = T_c$ ) and with the HTSE (dashed, black) [6] close to  $\tau = 1$  ( $T \rightarrow \infty$ ) as well as with the MCHTSE estimates in between.

the critical temperatures at each value of  $d$  are given later in this section and listed in Tables 1 and 2. Accepting this more accurate estimate for  $d = 5$ , a fit to the remaining five parameters yields an estimate for  $\gamma$  of 1.0(2). Accepting the mean field value  $\gamma = 1$  and fitting to the remaining four parameters gives  $\Gamma = 1.28(2)$ ,  $B = -0.44(19)$ , so that  $1 - \Gamma - B = 0.16(21)$ , which is compatible with  $C = 0.17(21)$ . Accepting that  $C = 1 - \Gamma - B$  (i.e., using extended scaling), a three-parameter fit to the amplitudes  $\Gamma$  and  $B$ , as well as to the correction exponent gives  $\vartheta = -0.47(8)$ . Finally, accepting that  $\vartheta$  is, in fact  $-0.5$ , as in (2.3), a two-parameter fit to the amplitudes of the leading and first correction terms gives  $\Gamma = 1.291(3)$  and  $B = -0.310(8)$ . The goodness of fit for each of these measurements (and for each fit reported below) is monitored through the chi-squared per degree of freedom and is observed to be reasonable in each case. These results, together with the higher dimensional ones, are summarized in Table 2, where the refined (see below) extended scaling estimates for the critical temperature are also given.

The same analysis applied to the  $L = 16$  MCHTSE data yields very similar results and, in particular,  $\Gamma = 1.291(3)$ ,  $B = -0.311(8)$ . For comparison, Guttman's series analysis yielded  $\Gamma = 1.311(9)$  and  $B = -0.480(30)$  [4].

This extended scaling (i.e., (2.9) with  $C(\tau) = C = 1 - \Gamma - B$  and  $\Gamma = 1.291(3)$  and  $B = -0.311(8)$ ) is depicted in Fig. 3 for the  $d = 5$  case. This line coincides with the HTSE [6] for high temperature ( $\tau \rightarrow 1$ ) and with the critical expansion [4] close to  $T_c$  ( $\tau = 0$ ). Between these extremes, it successfully follows the MCHTSE data. It is clear from Fig. 3 that the critical reduced-temperature line of [4] deviates significantly from the

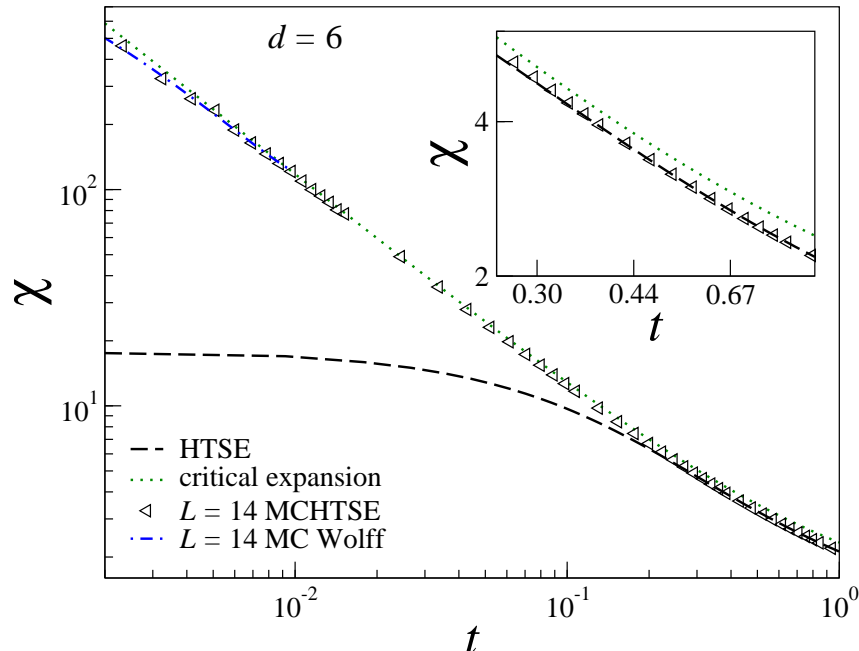


Figure 4: MCHTSE estimates for the susceptibility of the six-dimensional Ising model compared with estimates coming from conventional Monte Carlo (dot-dashed, blue online), the HTSE of [6] (dashed, black) and the critical expansion of [4] (dotted, green online). The inset illustrates the deviation of the critical expansion from the HTSE at high temperature.

data away from  $T_c$ , a circumstance typically ascribed to correction terms. Similarly the HTSE curve deviates from the data as the temperature is reduced. On the other hand, the reduced temperature curve nicely follows the critical expansion for small  $\tau$  and the data to very large  $T$ . Thus the extended scaling method proposed in [1] is indeed seen to be superior to the conventional approach, also in high dimensions.

In summary, the extended scaling analysis of the MCHTSE data yields similar but improved results to that of [4] for the  $d = 5$  Ising susceptibility. Therefore, confidence has been established in the method, which can now be applied to higher dimensions to determine critical parameters which were unobtainable previously.

## 4.2 Six-dimensional case

In Fig. 4, the six-dimensional  $L = 14$  MCHTSE data are compared with the HTSE and the critical expansion as well as conventional (reweighted)  $L = 14$  MC data. Similar to the five-dimensional case, the MCHTSE data follow the critical curve close to  $t = 0$  and switches to the HTSE curve for larger  $t$ . The inset of Fig. 4 illustrates the deviation of the critical curve from the HTSE and the MCHTSE data.

Although the leading correction term in six dimensions is expected to involve a logarithm after (2.4), we initially fit to the form (4.1) so as not to a priori bias in favor of the

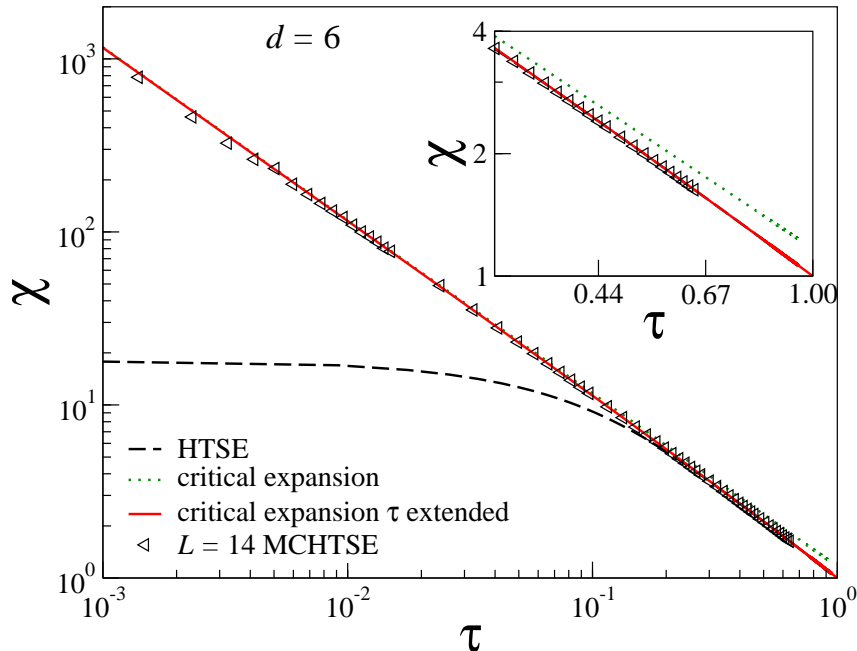


Figure 5: Extended scaling for the susceptibility of the Ising model in  $d = 6$  dimensions. The extended scaling curve (solid, red line) traces the critical curve of [4] (dotted, green online) close to  $\tau = 0$  and the HTSE [6] (dashed) close to  $\tau = 1$  and as with the MCHTSE estimates in between.

logarithmic structure. Using the MCHTSE data for  $L = 14$ , and fitting to 55 data points from  $T = 10.88$  to  $T = 30$ , a six-parameter fit to the form (4.1) gives  $T_c = 10.8318(24)$ , close to the value  $T_c = 10.8348(4)$  measured in [6]. Following the same procedure as in the five-dimensional case, and accepting this value, subsequent fits yield  $\gamma = 0.95(25)$  and  $\vartheta = -0.01(40)$ . Since the latter value is close to zero (and because the fitting process becomes more unstable as the number of parameters is reduced), we conclude that a logarithmic term may indeed be present at the leading-correction level.

We therefore perform a four-parameter fit to the form (2.10) which gives  $\gamma = 0.994(3)$ . Accepting the mean field value  $\gamma = 1$ , a three-parameter fit gives  $1 - \Gamma = -0.1607(24)$  and  $C = -0.1605(18)$ . Accepting that  $C = 1 - \Gamma$  (extended scaling) then yields  $\Gamma = 1.1606(17)$  and  $B = 0.0571(27)$ . The value for  $\Gamma$  compares well with Guttman's estimate 1.168(8) [4]. The logarithmic term was not addressed in previous analysis [4, 6].

Extended scaling (i.e., (2.10) with  $\Gamma = 1.1606(17)$ ,  $B = 0.0571(27)$  and  $C = 1 - \Gamma$ ) is depicted in Fig. 5 for the  $d = 6$  case. This line coincides with the HTSE [6] for high temperature ( $\tau \rightarrow 1$ ) and with the critical expansion [4] close to  $T_c$  ( $\tau = 0$ ) and traces the MCHTSE data in between.

### 4.3 Seven-dimensional case

For  $d = 7$  dimensions, we simulated at three different lattice sizes ( $L = 10, 12$  and  $14$ ) to again determine the temperature range over which the MCHTSE data are  $L$  independent

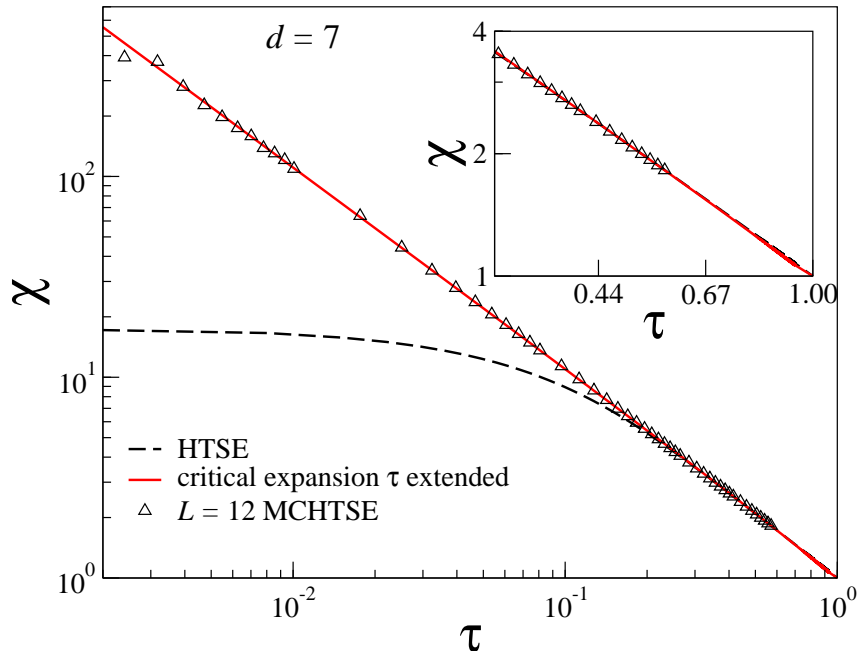


Figure 6: Extended scaling (solid curve, red online) for the susceptibility of the Ising model in  $d = 7$  dimensions with the HTSE of [6] (dashed curve, black online) and the MCHTSE data.

( $T = 12.89$ – $30$ ). Fitting the  $L = 12$  data to all four parameters in (2.11) yields  $T_c = 12.8665(5)$ , close to the value  $12.8690(4)$  (obtained in [6] using the HTSE), which we now accept (pending our refined extended scaling estimate, which we give below). A three-parameter fit then yields  $\gamma = 1.000(2)$ , and accepting the mean field value  $\gamma = 1$ , we find  $\Gamma = 1.1086(9)$  and  $C = -0.1215(20)$ . Accepting that  $C = 1 - \Gamma$  (extended scaling) finally gives  $\Gamma = 1.1008(5)$ . The extended scaling plot for seven dimensions is given in Fig. 6.

#### 4.4 Eight-dimensional case

A similar analysis in eight dimensions (with  $L = 8$ ) gives the successive estimates  $T_c = 14.8893(20)$  (to be compared with the value  $T_c = 14.893(3)$  from finite-size scaling [13]),  $\gamma = 0.998(2)$ ,  $\Gamma = 1.0935(45)$  and  $C = -0.0950(26)$ . Extended scaling ( $C = 1 - \Gamma$ ) then yields  $\Gamma = 1.0836(5)$ . The extended scaling plot for  $d = 8$  is depicted in Fig. 7, where it too is compared with the HTSE [6] and the critical expansion [4]. These results, with refined estimates for the critical temperature, are summarized in Table 2.

Having established that  $\gamma = 1$  in each case, and the expected scaling forms (2.3) to (2.6) indeed hold, we return to the estimates of  $T_c$  in each dimension. Refitting to these forms for the critical temperature (as well as the amplitudes) yields the more refined estimates  $T_c = 8.7777(9)$ ,  $T_c = 10.8353(4)$ ,  $T_c = 12.8690(3)$ ,  $T_c = 14.8933(8)$ , for  $d = 5$ ,  $d = 6$ ,  $d = 7$  and  $d = 8$  respectively. These values should be compared with previous estimates in the literature, which are listed in Table 1.

With the Boltzmann constant and the coupling strength having both been set to

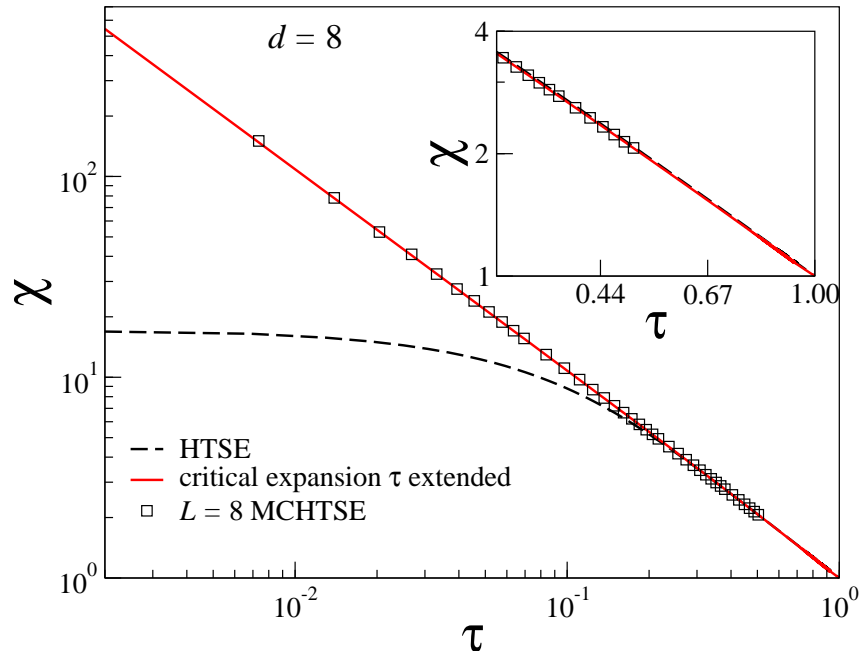


Figure 7: Extended scaling curve (solid, red online) for the Ising susceptibility in  $d = 8$  dimensions with the HTSE of [6] (dashed curve, black online) and the MCHTSE data.

unity, for a regular lattice of the type considered here the mean field expressions for the Ising critical temperature and amplitude are  $T_c = 2d$  and  $\Gamma = 1$ . The results for  $T_c$  and  $\Gamma$ , summarized in Table 2, illustrate this approach to these classical values as the dimensionality is increased. The approach to mean field is also illustrated in Fig. 8, using our estimates for  $T_c$  for  $d = 5$  to  $d = 8$  together with the exact result for  $d = 2$  [20] and best estimates from the literature for  $d = 3$  and  $d = 4$  [21, 22]. These data are fitted to polynomials of increasing degree in  $1/d$  until the goodness of fit becomes reasonable. The solid curve represents a fit to the polynomial form  $\beta_c = b_1/d + b_2/d^2 + b_3/d^3 + b_4/d^4$ , with  $b_1 = 0.5044(3)$ ,  $b_2 = 0.1935(30)$ ,  $b_3 = 0.3540(101)$  and  $b_4 = 1.5335(104)$ . The dashed line represents the mean field approximation  $T_c = 2d$ .

## 5 Conclusions

We have presented estimates for the magnetic susceptibility in the paramagnetic phase of high-dimensional Ising models, obtained using the Prokof'ev-Svistunov worm algorithm which enables the stochastic generation of the HTSE by Monte Carlo methods. The resulting data are checked against the critical expansion [4], the HTSE [6] and the results of a standard Monte Carlo approach using the Wolff algorithm [18]. When applied to this data, the new extended scaling approach of [1] is demonstrated to work well in  $d = 5$  dimensions, where known results for the estimates of critical parameters [4] are recovered and improved. Having thus established confidence in the extended scaling approach above the upper critical dimension, it is then applied to the data obtained in  $d = 6$ ,  $d = 7$  and

Table 2: Summary of the numerical results obtained in this paper for dimensions  $d = 5$  to  $d = 8$ . The leading exponent is compatible with the mean field result  $\gamma = 1$ . In  $d = 6$  dimensions, the leading correction is logarithmic. Analytic corrections dominate confluent exponents beyond  $d = 6$ .

$d$	$T_c$	$\gamma$	$\vartheta$	Amplitudes
5	8.7777(9)	1.0(2)	-0.47(8)	$\Gamma = 1.291(3)$ , $B = -0.310(8)$ $C = 0.019(11)$
6	10.8353(4)	0.994(3)	0 [logarithm]	$\Gamma = 1.1606(17)$ , $B = 0.0571(27)$ $C = -0.1606(17)$
7	12.8690(3)	1.000(2)		$\Gamma = 1.1008(5)$ , $C = -0.1008(5)$
8	14.8933(8)	0.998(2)		$\Gamma = 1.0836(5)$ , $C = -0.0836(5)$

$d = 8$  dimensions to deliver estimates for critical parameters (especially those governing confluent corrections) there. In particular, the logarithmic correction in six dimensions (unobtainable in previous analyses [4, 6]) is clearly verified. It is also observed how the infinite dimensional ( $d \rightarrow \infty$ ) limit leads to the mean field theory. In this way, the general formula (2.2) is supported for the Ising model and a full account of the leading and confluent corrections to scaling in the odd sector above the upper critical dimension is given.

**Acknowledgements:** The laboratoire de Physique des Matériaux is Unité Mixte de Recherche CNRS number 7556. We wish to thank Paolo Butera and Ian Campbell for e-mail correspondences.

## References

- [1] I.A. Campbell, K. Hukushima and H. Takayama, Phys. Rev. Lett. **97** (2006) 117202; Phys. Rev. B **76** (2007) 134421.
- [2] I.A. Campbell and P. Butera, Phys. Rev. B **78** (2008) 024435.
- [3] H.G. Katzgraber, I.A. Campbell and A.K. Hartmann, arXiv:0809.1161.
- [4] A.J. Guttmann, J. Phys. A, **14** (1981) 233.
- [5] G.S. Joyce, in *Phase Transitions and Critical Phenomena*, ed. C. Domb and M.S. Green, Vol. 2 (Academic Press, London, 1972).
- [6] M. Gofman, J. Adler, A. Aharony, A.B. Harris and D. Stauffer, J. Stat. Phys. **71** (1993) 1221.

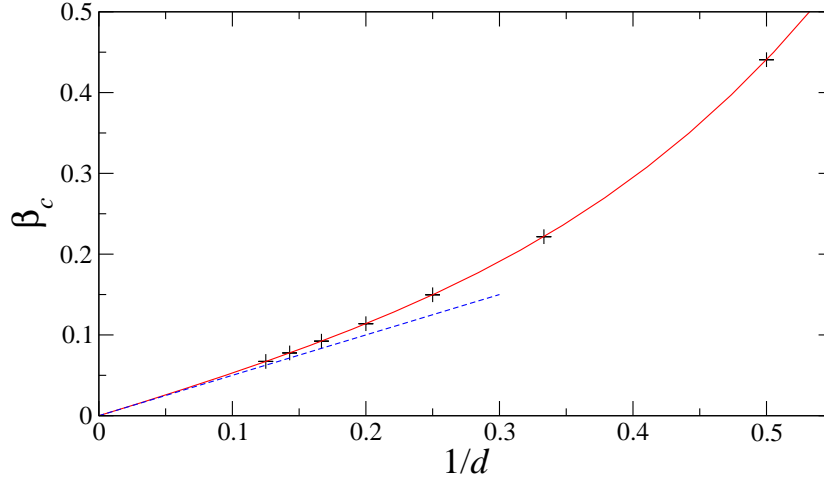


Figure 8: The approach of the critical temperature (solid curve, red online) to the classical mean field value (dashed line, blue online) with increasing dimensionality.

- [7] C. Münkler, D.W. Heermann, J. Adler, G. Gofman and D. Stauffer, *Physica A* **193** (1993) 540.
- [8] M.E. Fisher and D.S. Gaunt. *Phys. Rev. A* **133** (1964) 224.
- [9] E. Luijten, K. Binder and H.W.J Blöte, *Eur. Phys. J. B* **9** (1999) 289; N. Aktekin, Ş. Erkoç and M. Kalay, *Int. J. Mod. Phys. C* **10** (1999) 1237.
- [10] N. Aktekin and Ş. Erkoç, *Physica A* **284** (2000) 206; Z. Merdan and M. Bayırh, *Applied Mathematics and Computation* **167** (2005) 212; Z. Merdan and R. Erdem, *Phys. Lett. A* **330** (2004) 403.
- [11] N. Aktekin and Ş. Erkoç, *Physica A* **290** (2001) 123; Z. Merdan and D. Atille, *Physica A* **376** (2007) 327.
- [12] J.L. Jones and A.P. Young, *Phys. Rev. B* **71** (2005) 174438.
- [13] Z. Merdan, A. Duran, D. Atille, G. Mülazimoğlu and A. Günen, *Physica A* **366** (2006) 265.
- [14] N. Prokof'ev and B. Svistunov, *Phys. Rev. Lett.* **87** (2001) 160601.
- [15] U. Wolff, arXiv:0808:3934.
- [16] Y. Deng, T.M. Garoni and A.D. Sokal, *Phys. Rev. Lett.* **99** (2007) 110601.
- [17] A.B. Bortz, H. Kalos and J.L. Lebowitz, *J. Comp. Phys.* **17** (1975) 10.

- [18] U. Wolff, Phys. Rev. Lett. **62** (1989) 361.
- [19] A. M. Ferrenberg and R. H. Swendsen, Phys. Rev. Lett. **61** (1988) 2635; *ibid.* **63** (1989) 1195.
- [20] H.A. Kramers and G.H Wannier, Phys. Rev. **60** (1941) 252.
- [21] Y. Deng and H.W.J. Blöte, Phys. Rev. E **68** (2003) 036125.
- [22] R. Kenna and C.B. Lang, Phys. Lett. B **264** (1991) 396; Nucl. Phys. B **393** (1993) 461.